

# A Tutorial Introduction to Very Long Baseline Interferometry (VLBI) Using Bandwidth Synthesis

J. I. Molinder

TDA Engineering and Harvey Mudd College

*This article gives a tutorial presentation of the basic principles underlying Very Long Baseline Interferometry (VLBI) using bandwidth synthesis. Although many subtle details are ignored, the article presents the basic signal processing approach and summarizes results showing the tradeoff of measurement accuracy with spanned bandwidth, source strength, antenna size and efficiency, system noise temperature, and data volume. Results pertaining to minimization of required antenna time for a given baseline measurement accuracy are also discussed.*

## I. Introduction

A concise description of VLBI, given in Ref. 1, is repeated below.

In very long baseline interferometer (VLBI) measurements, the radio signal produced by a distant source is recorded simultaneously at two radio antennas. Because of a difference in raypaths, the signal will be delayed in time at one antenna relative to the other. By cross correlating the two signals, the time delay and/or its time derivative may be determined. In addition, correlated amplitude measurements can yield source strength and structure. If the radio signal is generated by an extragalactic object, the radio source may be regarded as a fixed object because of its great distance. In this case, the time dependence of the time delay is generated by the Earth's motion but depends, of course, on the source location and the baseline vector between the two antennas. In general, measurement of the time delay

and/or its derivative for many sources can lead to a least-squares determination of source locations, the baseline vector, and Earth motion parameters, such as UT1 and polar motion.

Although much has been written about VLBI, a need was felt for a tutorial introduction to the basic principles involved. It is much easier to understand the more detailed analyses of VLBI after the central ideas are understood. Thus this tutorial concentrates only on the basic principles and ignores many subtle details that are discussed thoroughly in the literature.

## II. Monochromatic Source (Ref. 2)

Consider two antennas separated by a distance (baseline)  $B$  receiving a signal from a distant extraterrestrial source. The geometry is shown in Fig. 1. If the source is assumed to be monochromatic and noise (receiver and background) is

neglected, the received signals at the two antennas can be represented as

$$V_1(t) = A_1 \cos 2\pi f_s t$$

and

$$V_2(t) = A_2 \cos 2\pi f_s (t - \tau_g) \quad (1)$$

where

$A_1, A_2$  represent the strength of the received signals at antennas 1 and 2, respectively

$\tau_g = (B \cos \psi)/c$  is the time delay (typically a slowly varying function of time due to the earth's rotation) in the reception of a given wavefront at antenna 2 relative to antenna 1

$c$  is the velocity of light

These signals are processed by the system shown schematically in Fig. 2 to produce a cross-correlation function  $R(\tau_g, \tau_m, t)$ . From Fig. 2,

$$\begin{aligned} V_{im}(t) &= [A_1 \cos 2\pi f_s t] [M_1 \cos (2\pi f_{LO1} t - \theta_1)] \\ &= \frac{A_1 M_1}{2} \cos [2\pi(f_s - f_{LO1})t + \theta_1] \\ &\quad + \frac{A_1 M_1}{2} \cos [2\pi(f_s + f_{LO1})t - \theta_1] \end{aligned} \quad (2)$$

where

$f_{LO1}$  is the effective local oscillator mixing frequency at station 1

$M_1$  is the amplitude of the local oscillator at station 1

$\theta_1$  represents phase shifts due to the receiver and local oscillator (Phase shifts due to other propagation effects such as the ionosphere can also be included in this term.)

The low-pass filter is designed to pass the difference term and reject the sum term. (Assume for simplicity that the filter gain is 1 for the difference frequency. Equivalently it can be lumped in with  $M_1$  and  $\theta_1$ .) Thus the recorded signal at station 1 is given by

$$V_{1L}(t) = \frac{A_1 M_1}{2} \cos [2\pi(f_s - f_{LO1})t + \theta_1] \quad (3)$$

In an entirely similar fashion,

$$V_{2L}(t) = \frac{A_2 M_2}{2} \cos [2\pi(f_s - f_{LO2})t - 2\pi f_s \tau_g + \theta_2] \quad (4)$$

As indicated in Fig. 2,  $V_{1L}(t)$  and  $V_{2L}(t)$  are typically recorded on magnetic tape (digitally in most cases, as discussed later) and shipped to a central facility for correlation and further processing.

Correlation consists of advancing the recorded signal  $V_{2L}(t)$  from station 2 by a model time  $\tau_m$  that approximates the expected geometric delay  $\tau_g$ , taking the product of the signals and again low-pass filtering. This is equivalent to multiplying  $V_{1L}(t)$  and  $V_{2L}(t + \tau_m)$  and low-pass filtering. From Eq. (4),

$$\begin{aligned} V_{2L}(t + \tau_m) &= \frac{A_2 M_2}{2} \cos [2\pi(f_s - f_{LO2})(t + \tau_m) - 2\pi f_s \tau_g + \theta_2] \\ &= \frac{A_2 M_2}{2} \cos [2\pi(f_s - f_{LO2})t \\ &\quad + 2\pi(f_s - f_{LO2})\tau_m - 2\pi f_s \tau_g + \theta_2] \end{aligned} \quad (5)$$

Taking the product of  $V_{1L}(t)$  and  $V_{2L}(t + \tau_m)$ , expanding into sum and difference terms, and noting that the low-pass filter removes the sum (high-frequency) term yields

$$R(\tau_g, \tau_m, t) = K \cos \phi_f(t) \quad (6)$$

where

$$K = \frac{A_1 A_2 M_1 M_2}{8}$$

and

$$\begin{aligned} \phi_f(t) &= 2\pi(f_{LO2} - f_{LO1})t - 2\pi(f_s - f_{LO2})\tau_m \\ &\quad + 2\pi f_s \tau_g + \theta_1 - \theta_2 \end{aligned}$$

The cross-correlation function  $R(\tau_g, \tau_m, t)$  is processed further (as will be discussed in a later section) and the delay  $\tau_g$  as well as the delay rate  $\dot{\tau}_g$ , which are the basic VLBI data types, are determined by analyzing the phase of the cross-correlation function. Note that  $\phi_f(t)$  may also be written in the form

$$\begin{aligned} \phi_f(t) &= 2\pi(f_{LO2} - f_{LO1})t + 2\pi f_s \Delta\tau \\ &\quad + 2\pi f_{LO2} \tau_m + \theta_1 - \theta_2 \end{aligned} \quad (7)$$

where

$$\Delta\tau = \tau_g - \tau_m$$

### A. Angular Sensitivity

The geometric delay  $\tau_g$  enters into the phase of the cross-correlation function  $\phi_f(t)$  as the term  $2\pi f_s \tau_g$ . Suppose it is possible to detect a variation in the phase  $\phi_f(t)$  of  $2\pi$  radians (a one-fringe change). This corresponds to a change in geometric delay (assuming the other terms of  $\phi_f(t)$  do not change) given by

$$2\pi f_s \Delta\tau_g = 2\pi \quad (8)$$

or

$$\Delta\tau_g = \frac{1}{f_s}$$

Now the relationship between small changes in  $\tau_g$  and small changes in the angle to the source  $\psi$  can be approximated by

$$\Delta\tau_g \cong \frac{\partial\tau_g}{\partial\psi} \Delta\psi \quad (9)$$

Substituting  $\tau_g = (B \cos \psi)/c$  yields

$$\Delta\tau_g = \frac{-B \sin \psi}{c} \Delta\psi \quad (10)$$

or

$$\Delta\psi = \frac{-c}{B \sin \psi} \Delta\tau_g$$

Using  $\Delta\tau_g = \frac{1}{f_s}$  gives

$$\Delta\psi \cong \frac{-c}{B \sin \psi} \frac{1}{f_s} = \frac{-\lambda}{B \sin \psi} \quad (11)$$

since  $c/f_s = \lambda$ , where  $\lambda$  is the wavelength of radiation at frequency  $f_s$ .

As an example, suppose  $B = 10,000$  km and  $\lambda = 13$  cm (corresponding to an S-band signal). Then

$$\Delta\psi \cong \frac{-1.3 \times 10^{-1}}{1 \times 10^7 \sin \psi} = \frac{-1.3 \times 10^{-8}}{\sin \psi} \text{ rad}$$

$$= \frac{-0.0027}{\sin \psi} \text{ arc sec} \quad (12)$$

As stated in Ref. 2, "This illustrates the potential of VLBI: a change in position of  $10^{-3}$  arc sec causes detectable changes in the cross correlation. At the present though, there is an ambiguity in determining which fringe the source is on." That ambiguity problem is brought out in the next two sections.

### B. Phase Measurement

The cross-correlation function  $R(\tau_g, \tau_m, t)$  is multiplied by the cosine and sine of a model phase  $\phi_m(t)$  and integrated over an interval of  $T$  seconds (the integrator eliminates the sum frequency term of the product) to produce the so-called cosine and sine-stopped fringes

$$\mu_c(t, \tau_m) = \frac{K}{2} \cos [\phi_f(t) - \phi_m(t)]$$

and

$$\mu_s(t, \tau_m) = \frac{K}{2} \sin [\phi_f(t) - \phi_m(t)] \quad (13)$$

The phase of the cross-correlation function can, in principle, be determined (within a multiple of  $2\pi$ ) as

$$\phi_f(t) - \phi_m(t) = \tan^{-1} \frac{\mu_s(t, \tau_m)}{\mu_c(t, \tau_m)}$$

or

$$\phi_f(t) = \phi_m(t) + \tan^{-1} \frac{\mu_s(t, \tau_m)}{\mu_c(t, \tau_m)} \quad (14)$$

In actual practice the phase is determined by fitting sinusoids to the cosine and sine-stopped fringes.

### III. Polychromatic Source and Bandwidth Synthesis

As noted above, the phase of the cross-correlation function  $R(\tau_g, \tau_m, t)$  due to geometric delay can be determined only within a multiple of  $2\pi$  (i.e.,  $\phi_f(t) = 2\pi f_s \tau_g + 2\pi n$ ). If the source consists of several spectral lines (polychromatic) it is possible to determine the delay by combining measurements from the cross-correlation functions of the individual spectral lines. As an example, suppose the source consists of two spectral lines at frequencies  $f_{s1}$  and  $f_{s2}$ . The phases of the cross-correlation functions due to the geometric delay term are then measured as

$$\phi_{f_1}(t) = 2\pi f_{s_1} \tau_g + 2\pi m$$

and

$$\phi_{f_2}(t) = 2\pi f_{s_2} \tau_g + 2\pi n \quad (15)$$

where  $m$  and  $n$  are integers (see Fig. 3). If the a priori uncertainty in slope  $S$  of phase versus frequency is less than  $\Delta S_{1,2} = 2\pi/(f_{s_2} - f_{s_1})$ , then corresponding phase points may be connected (i.e., the relative phase ambiguity resolved) and the delay  $\tau_g$  is determined by the slope of the connecting line, since

$$\tau_g = \frac{\phi_{f_2} - \phi_{f_1}}{2\pi(f_{s_2} - f_{s_1})}$$

or

$$\tau_g = \frac{S}{2\pi} \quad (16)$$

It is important to note that the uncertainty in  $S$  includes uncertainties in both  $\tau_g$  and instrumental delays. The instrument delay uncertainty can be essentially eliminated by using a phase calibrator. In addition, there is of course some uncertainty in the measurement of the phase  $\phi_f(t)$  due to noise as indicated by the error bars in Fig. 3. (Noise is considered in a later section.) If the uncertainty in the measurement of  $\phi_f(t)$  at a given frequency is  $\sigma_{\phi_f}$ , then the uncertainty in  $\tau_g$  (neglecting certain errors due to ionospheric effects) is given by

$$\sigma_{\tau_g} = \frac{\sqrt{2} \sigma_{\phi_f}}{2\pi(f_{s_2} - f_{s_1})} \quad (17)$$

where the  $\sqrt{2}$  results from incoherent differencing of phase errors. The point is that for a given  $\sigma_{\phi_f}$ , the larger the term  $f_{s_2} - f_{s_1}$  (commonly called the spanned bandwidth), the smaller will be the delay uncertainty  $\sigma_{\tau_g}$ . This technique is known as bandwidth synthesis.

In this simple example, increasing the spanned bandwidth would also require more accurate a priori information in order to resolve the relative phase ambiguity. This dilemma can be avoided if an additional intermediate channel is added as shown in Fig. 3. Assume the relative phase ambiguity is resolved between channels 1 and 3 using a priori information. The more precise estimate of  $\tau_g$  determined by using channels 1 and 3 may now be used to resolve the ambiguity between the outside channels 1 and 2. Obviously several intermediate channels may be required to resolve the relative phase

ambiguities depending on the spanned bandwidth, accuracy of the a priori information, and uncertainty in individual phase measurements.

## IV. Wideband Source and Noise

### A. Cross-Correlation Function

In most cases the source used in VLBI (a natural radio source for example) is broadband and can be approximated as white noise over the band of interest. In this case the correlation function can be shown (Ref. 1) to be of the form

$$R(\tau_g, \tau_m, t) = D(\Delta\tau) \cos \phi_f(t) \quad (18)$$

where

$$\Delta\tau = \tau_g - \tau_m$$

$$\phi_f(t) = 2\pi(f_{LO2} - f_{LO1})t + 2\pi f_s \Delta\tau + 2\pi f_{LO2} \tau_m + \theta_1 - \theta_2$$

Note that the correlation function differs from the monochromatic case in that the amplitude of the correlation function  $D(\Delta\tau)$  is a function of  $\Delta\tau = \tau_g - \tau_m$  rather than a constant. For example, if the receiver has a rectangular bandpass of width  $W$  centered at  $f_s$ , the amplitude of the correlation function is given by (Ref. 1)

$$D(\Delta\tau) = K_1 W \frac{\sin \pi W \Delta\tau}{\pi W \Delta\tau} \quad (19)$$

where  $K_1$  is a constant. This dependence on model delay reflects the accuracy with which the two signals have been aligned in time.

Note further that, in the case of a broadband source, delay information can be obtained by analyzing the amplitude as well as the phase of the cross-correlation function. To determine  $\tau_g$  from the amplitude of the cross-correlation function, the model delay  $\tau_m$  is adjusted to maximize  $D(\Delta\tau)$ , at which point  $\Delta\tau = \tau_g - \tau_m = 0$  or  $\tau_g = \tau_m$ .

The accuracy with which delay can be determined using the amplitude of the cross-correlation function depends on the width of the peak of  $D(\Delta\tau)$  versus  $\Delta\tau$ . In the case of a rectangular bandpass, the first zero of  $D(\Delta\tau)$  (see Fig. 4) occurs at  $\pi W \Delta\tau = \pi$  or  $\Delta\tau = 1/W$ . Thus the accuracy with which delay can be determined using this technique is proportional to the reciprocal of the channel bandwidth. Typically this bandpass shape can be used to estimate the delay  $\tau_g$  with

an accuracy of  $0.01/2W$  to  $0.1/2W$  seconds (2.5 to 25 nsec for  $W = 2\text{MHz}$ ).

## B. Bandwidth Synthesis

Rather than use the amplitude of the cross-correlation function to determine the delay, which would require recording a wide-bandwidth signal, several narrower bandwidth channels are used (see Fig. 5). Cross-correlation functions are computed for each channel, and the delay is determined by analyzing the phases of the cross-correlation functions and using bandwidth synthesis as explained above for the polychromatic source. However, the amplitude of the single-channel cross-correlation function can be used to improve a priori knowledge of  $\tau_g$  prior to performing bandwidth synthesis. It can be shown that for a given delay uncertainty  $\sigma_{\tau_g}$ , bandwidth synthesis requires less data than the amplitude technique for many cases of practical interest (Ref. 3).

J. B. Thomas has drawn up an alternate way of looking at the bandwidth synthesis process shown schematically in Fig. 6. First of all, the amplitude of the correlation function is used to give an unambiguous delay measurement based on the channel bandwidth  $W$  (2 MHz in this case). This delay measurement can then be used to resolve the delay ambiguity resulting from the most closely spaced channel pair (5 MHz in this example). The delay ambiguity results from the phase slopes spaced by  $\Delta S_{1,3}$  in Fig. 3 [ $\Delta\tau_{1,3} = (1/2\pi) \Delta S_{1,3}$ ]. Once the ambiguity in the most closely spaced channel pair is resolved, the more accurate measured delay obtained is in turn used to resolve the ambiguity in the more widely spaced channel pair (20 MHz in this case). Note, that both the uncertainty in the delay measurement and the ambiguity spacing decrease as the channel separation increases (see Eqs. 16 and 17) as indicated in Fig. 6.

## V. Effect of Noise and Digital Processing

When noise is included, the cross-correlation function may be written

$$R(\tau_g, \tau_m, t) = D(\Delta\tau) \cos \phi_f(t) + n(t) \quad (20)$$

where  $n(t)$  is a random function due to receiver and background noise. A rather involved analysis (Refs. 4 and 5) shows that

$$\frac{S}{N} = \frac{D(\Delta\tau)_{\max}}{\sigma_n} = \frac{D(0)}{\sigma_n} = \sqrt{\frac{T_{a1} T_{a2} WT}{T_{s1} T_{s2}}} \quad (21)$$

where

$$\frac{S}{N} = \text{stopped fringe signal-to-noise ratio}$$

$$\sigma_n = \text{rms fringe noise}$$

$$T_{a1}, T_{a2} = \text{effective radio source temperatures (K) at stations 1 and 2, respectively}$$

$$T_{s1}, T_{s2} = \text{total system noise temperature (K) at stations 1 and 2, respectively}$$

$$W = \text{channel bandwidth (Hz)}$$

$$T = \text{total integration time (sec)}$$

In the actual implementation of this technique each channel is hard-limited and sampled (1-bit quantization) at a rate  $2W$ . The effect of hard-limiting for low signal-to-noise ratios is to reduce the signal to noise ratio  $S/N$  by a factor of  $2/\pi$  (Ref. 4) and thus for the actual system

$$\frac{S}{N} = \frac{2}{\pi} \sqrt{\frac{T_{a1} T_{a2} WT}{T_{s1} T_{s2}}} \quad (22)$$

Note that maximum  $S/N$  requires that the model delay  $\tau_m$  must be accurate enough to keep  $D(\Delta\tau)$  near its maximum  $D(0)$  to provide the most accurate measurement in the presence of noise as described below. In addition, further processing requires "seeing" fringes, which in practice requires that  $S/N$  be at least 5 and preferably 10.

## A. Phase and Delay Measurement Accuracy (Refs. 5 and 6)

The error in determining  $\phi_f(t) - \phi_m(t)$  from the stopped fringes may be illustrated by noting that  $\mu_c(t, \tau_m)$  and  $\mu_s(t, \tau_m)$  are projections of a vector consisting of the signal vector plus a noise vector on two orthogonal axes as shown in Fig. 7, where

$$\mu_c(t, \tau_m) = \frac{D(0)}{2} \cos [\phi_f(t) - \phi_m(t)] + \frac{n_c(t)}{2}$$

and

$$\mu_s(t, \tau_m) = \frac{D(0)}{2} \sin [\phi_f(t) - \phi_m(t)] + \frac{n_s(t)}{2} \quad (23)$$

Since the noise is spherically symmetric, it follows (see Fig. 7) that for small rms phase deviations,

$$\sigma_{\phi_f} = \tan^{-1} \left( \frac{\text{noise}}{\text{signal}} \right) \cong \frac{\text{noise}}{\text{signal}} = \frac{1}{S/N} = \frac{N}{S} \quad (24)$$

A more rigorous analysis (Ref. 5) yields the same result, and thus (assuming the relative phase ambiguities have been resolved) the system noise-limited delay accuracy  $\sigma_{\tau_g}$  is given by

$$\sigma_{\tau_g} = \frac{\sqrt{2} \sigma_{\phi_f}}{2\pi(f_{s2} - f_{s1})} \quad (25)$$

where  $f_{s1}$ ,  $f_{s2}$  now refer to the center frequencies of channels 1 and 2, respectively. Defining the spanned bandwidth  $B_s = f_{s2} - f_{s1}$  yields

$$\sigma_{\tau_g} = \frac{\sqrt{2} \sigma_{\phi_f}}{2\pi B_s} = \frac{\sqrt{2}}{4B_s} \sqrt{\frac{T_{s1} T_{s2}}{T_{a1} T_{a2} WT}} \quad (26)$$

Substituting (Ref. 7)

$$T_{ai} = \frac{1}{2} \frac{10^{-26}}{K} J \epsilon_i \frac{\pi}{4} d_i^2 \quad i = 1, 2 \quad (27)$$

where

$$\frac{1}{2} = \text{antenna polarization loss}$$

$$J = \text{correlated flux of radio source in Janskys (Jansky} = 10^{-26} \text{ W/m}^2 \text{ Hz)}$$

$$\epsilon_i = \text{antenna efficiency}$$

$$d_i = \text{antenna diameter in meters}$$

$$K = \text{Boltzmann's constant (} K = 1.38 \times 10^{-23} \text{ Joule/Kelvin)}$$

gives

$$\sigma_{\tau_g} = \frac{1.24 \times 10^3}{B_s J d_1 d_2} \sqrt{\frac{T_{s1} T_{s2}}{\epsilon_1 \epsilon_2 WT}} \text{ sec} \quad (28)$$

It is sometimes convenient to give  $\sigma_{\tau}$  in cm by multiplying by the speed of light ( $3 \times 10^{10}$  cm/sec). If, in addition, the spanned bandwidth  $B_s$  is measured in MHz ( $10^6$  Hz) and if the sampling rate is twice the channel bandwidth so that the number of megabits of data  $N$  is given by

$$N = \frac{2WT}{10^6} \text{ Mbits} = S_r T$$

where

$$S_r = \text{mean sampling rate in megabits/sec for each channel}$$

$$T = \text{total integration time in seconds}$$

$$B_s = \text{spanned bandwidth in MHz}$$

Then

$$\sigma_{\tau_g} \text{ (cm)} = \frac{K_2}{B_s J d_1 d_2} \sqrt{\frac{T_{s1} T_{s2}}{\epsilon_1 \epsilon_2 S_r T}} \text{ cm} \quad (29)$$

where

$$B_s = \text{spanned bandwidth in MHz}$$

$$J = \text{correlated flux of radio source in Janskys}$$

$$\epsilon_i = \text{antenna efficiency } i = 1, 2$$

$$d_i = \text{antenna diameter in meters}$$

$$K_2 = 5.26 \times 10^4$$

Again it is important to note that Eq. (29) gives the standard deviation in the measurement of the delay  $\tau_g$  due to thermal noise only. Other error sources such as instrumental effects, propagation (ionosphere), modelling, etc., must also be considered. The real importance of the equation is to show the manner in which various parameters affect VLBI accuracy.

As an example, using the following values for a typical Mark II observation,

$$K_2 = 5.26 \times 10^4$$

$$J = 1 \text{ Jansky}$$

$$T_{s1} = T_{s2} = 30 \text{ K}$$

$$S_r = 4 \text{ Mbps}$$

$$B_s = 40 \text{ MHz}$$

$$d_1 = d_2 = 64 \text{ m}$$

$$\epsilon_1 = \epsilon_2 = 0.55$$

$$T = 150 \text{ sec (2-1/2 min)}$$

yields

$$\sigma_{\tau_g} \text{ (cm)} = \frac{5.26 \times 10^4}{(40)(1)(64)(64)} \sqrt{\frac{(30)(30)}{(0.55)(0.55)(4)(150)}} = 0.7 \text{ cm}$$

Note that if the spanned bandwidth and antenna parameters are held fixed,  $\sigma_{\tau_g}$  varies as  $(S_r T)^{-1/2} = N^{-1/2}$ , where  $N$  = total number of bits for the observation. In the above example,

$$N = S_r T = 4(150) = 600 \text{ Mbits} = 6 \times 10^8 \text{ bits}$$

The sampling rate  $S_r$  is proportional to the channel bandwidth (2 MHz for the Mark II VLBI system) and thus, if the channel bandwidth is increased, the integration time  $T$  can be decreased while maintaining a given  $\sigma_{\tau_g}$  as long as  $N = S_r T$  is held constant. A wider channel bandwidth may allow a more accurate single-channel delay to be computed, however, which affects the resolution of phase ambiguities in the bandwidth synthesis process.

It should also be pointed out that  $T$  refers to integration time, during which the same radio signal from the source is recorded at two stations. If short segments of the signal are recorded, careful timing is required to insure signal overlap.

## VI. Measurement of Source Position and Earth Motion Parameters

As stated in Ref. 1 for an extragalactic radio source, "the time dependence of the time delay is generated by the earth's motion but depends, of course, on the source location and the baseline vector between the two antennas." For example, the relationship between the geometric time delay  $\tau_g$ , baseline  $B$ , and source position is given by (Ref. 2)

$$\tau_g = \frac{B}{c} [\sin \delta \sin \delta_b + \cos \delta \cos \delta_b \cos (\alpha_b - \alpha)] \quad (30)$$

where

$B$  = length of the baseline

$\delta$  = declination of the source

$\delta_b$  = declination of the baseline

$\alpha$  = right ascension of the source

$\alpha_b$  = right ascension of the baseline

$c$  = velocity of light

In addition, the instantaneous spin axis of the earth (which is the reference for the source and baseline coordinates in Eq. 30 above) changes both with respect to an inertial reference frame (precession and nutation) and the earth's crust (polar motion).

A number of delay measurements at various times and for various sources can be used to make a least-squares determination of source coordinates, the baseline vector, and earth motion parameters. A discussion of some of the tradeoffs involved in this type of measurement is given in the next section using the baseline as an example.

### A. Baseline Accuracy

The standard deviation of the error in baseline measurement is approximately given by (Refs. 8 and 9)

$$\sigma = \sigma_x A \sqrt{\frac{N_p}{N_{\text{obs}}}} \quad (31)$$

where

$N_p$  = number of parameters solved for in the multi-parameter fit

$N_{\text{obs}}$  = number of observations

$A$  = constant ranging from 1 to 4 depending on a covariance analysis based on source locations, etc.

and

$$\sigma_x^2 = \sigma_{\tau_g}^2 + \sigma_o^2$$

where

$\sigma_{\tau_g}$  = that given previously

$\sigma_o$  = standard deviation of other uncertainties such as ionospheric effects, tropospheric effects, uncertainties in source positions (if taken as given), frequency standard deviations from linear performance in time, etc.

For example, consider solving for three earth parameters and four clock parameters using 28 observations, with  $\sigma_{\tau_g} = 0.7$  cm (see previous calculation) and  $A = 4$ . Assume for simplicity that  $\sigma_o = 0$ ; then

$$\sigma = (0.7)(4) \sqrt{\frac{7}{28}} = 1.4 \text{ cm}$$

The total number of bits required in this case is given by

$$N_T = N_{\text{obs}} S_r T = 28 \times 6 \times 10^8 = 1.68 \times 10^{10} \text{ bits}$$

## B. Delay Rate Accuracy

For a given standard deviation in phase  $\sigma_{\phi_f}$ , the standard deviation in delay rate may be approximated by noting that, from Eq. (6),

$$\dot{\phi}_f(t) = 2\pi f_s \dot{\tau}_g + 2\pi(f_{LO2} - f_{LO1}) \quad (32)$$

and thus

$$\sigma_{\dot{\phi}_f} = 2\pi f_s \sigma_{\dot{\tau}_g}$$

or

$$\sigma_{\dot{\tau}_g} = \frac{\sigma_{\dot{\phi}_f}}{2\pi f_s} \text{ sec/sec} \quad (33)$$

Since for an integration interval of  $T$  seconds,  $\dot{\phi}_f$  can be approximated by taking the difference in phase over the integration interval and dividing by  $T$ ,

$$\sigma_{\dot{\phi}_f} \cong \frac{\sqrt{2}\sigma_{\phi_f}}{T} \text{ radians/sec} \quad (34)$$

and thus

$$\sigma_{\dot{\tau}_g} = \frac{\sqrt{2}\sigma_{\phi_f}}{2\pi f_s T} \text{ sec/sec} \quad (35)$$

Note that there is no ambiguity problem in determining delay rate and the effective spanned bandwidth for delay rate is the rf channel frequency  $f_s$ . Since  $\sigma_{\phi}$  varies as  $T^{-1/2}$ ,  $\sigma_{\dot{\tau}_g}$  varies as  $T^{-3/2}$ . Note that although for a given spanned bandwidth and antenna parameters,  $\sigma_{\tau_g}$  depends only on the number of bits  $N = S_r T$  (thus allowing a tradeoff between integration time and channel bandwidth),  $\sigma_{\dot{\tau}_g}$  depends explicitly on the integration time  $T$  (varying as  $T^{-1}$  for a fixed  $\sigma_{\tau_g}$ ). From Eq. (26),

$$\sigma_{\phi_f} = \frac{2\pi B_s}{\sqrt{2}} \sigma_{\tau_g} \quad (36)$$

Substituting into Eq. (35),

$$\sigma_{\dot{\tau}_g} = \frac{B_s}{f_s T} \sigma_{\tau_g} \text{ sec/sec} \quad (37)$$

or

$$\sigma_{\dot{\tau}_g} = \frac{B_s}{f_s T} \sigma_{\tau_g} \text{ (cm) cm/sec}$$

Dividing by the wavelength of the signal at frequency  $f_s$ ,

$$\sigma_{\dot{\tau}_g} = \frac{B_s}{f_s T \lambda} \sigma_{\tau_g} \text{ (cm)} = \frac{B_s}{cT} \sigma_{\tau_g} \text{ (cm) Hz}$$

Using the previous Mark II example yields

$$\sigma_{\dot{\tau}_g} = \frac{40 \times 10^6}{(3 \times 10^{10})(150)} 0.7 = 6.22 \times 10^{-6} \text{ Hz}$$

Accurate measurement of  $\dot{\tau}_g$  strengthens the multiparameter fit for baseline measurement, especially the z-component (along the earth's rotation axis), as schematically indicated by Fig. 8. A tradeoff of  $\tau$  vs  $\dot{\tau}$  accuracy for a given baseline component accuracy thus exists. This affects observation strategy and has not been analyzed in detail as yet, since the experimental data on typical  $\sigma_{\dot{\tau}_g}$  at X-band are only now becoming available.

## VII. Required Antenna Time for a Given Baseline Accuracy

As discussed previously, the standard deviation of the error in baseline measurement is given by Eq. (31):

$$\sigma = \sigma_x A \sqrt{\frac{N_p}{N_{\text{obs}}}}$$

where

$$\sigma_x^2 = \sigma_{\tau_g}^2 + \sigma_o^2$$

and

$$\sigma_{\tau_g} = \frac{K_2}{B_s J d_1 d_2} \sqrt{\frac{T_{s1} T_{s2}}{\epsilon_1 \epsilon_2 S_r T}} \quad (38)$$

Following an analysis by D. Rogstad, the total antenna time  $T_{\text{ant}}$  and number of bits  $N_T$  required for a given baseline accuracy are given by

$$T_{\text{ant}} = N_{\text{obs}} (T + t_m) \quad (39)$$

and

$$N_T = N_{\text{obs}} S_r T \quad (40)$$

where  $t_m$  is the average time required to move from one source to another ( $\cong 4$  min for a 64-m/64-m antenna pair), and  $T$  is the integration time per source (assumed uniform). For convenience, define

$$\sigma_s = \frac{K_2}{B_s J d_1 d_2} \sqrt{\frac{T_{s1} T_{s2}}{\epsilon_1 \epsilon_2 S_r t_m}} \quad (41)$$

Then

$$\frac{\sigma_{\tau_g}}{\sigma_s} = \sqrt{\frac{t_m}{T}} \quad \text{or} \quad \sigma_{\tau_g}^2 = \sigma_s^2 \frac{t_m}{T} \quad (42)$$

and

$$\sigma^2 = (\sigma_{\tau_g}^2 + \sigma_o^2) \frac{A^2 N_p}{N_{\text{obs}}} = \left( \sigma_s^2 \frac{t_m}{T} + \sigma_o^2 \right) \frac{A^2 N_p}{N_{\text{obs}}} \quad (43)$$

Clearly, there is a tradeoff between  $T$  and  $N_{\text{obs}}$  in maintaining a constant  $\sigma$ . Rogstad has determined the minimum value

of  $T_{\text{ant}} = N_{\text{obs}}(T + t_m)$  subject to a constraint on  $\sigma$  (or  $\sigma^2$ ). The result (which can be derived using Lagrange multipliers) is

$$T_{\text{ant}} = N_p A^2 \left( \frac{\sigma_o}{\sigma} \right)^2 t_m \left( 1 + \frac{\sigma_s}{\sigma_o} \right)^2 \text{ sec}$$

This corresponds to

$$N_T = N_p A^2 \left( \frac{\sigma_o}{\sigma} \right)^2 S_r t_m \left( \frac{\sigma_s}{\sigma_o} \right) \left( \frac{\sigma_o}{s_D} + 1 \right) \text{ bits}$$

Normalized curves of the results are given in Ref. 9, as well as a discussion of how  $\sigma_o$  should be handled. Rogstad has subsequently obtained further results in this area.

## VIII. Summary

This tutorial is intended to give the reader an appreciation of the basic principles of VLBI. It should not be used as the sole basis of further analysis. A great deal of technical literature exists for those interested in further information and more detailed analyses. Especially recommended as a starting point are the articles by J. G. Williams (Ref. 2), A. E. E. Rogers (Ref. 10), and J. B. Thomas (Ref. 1, 4, and 11).

## Acknowledgements

The author is especially indebted to J. L. Fanselow and J. B. Thomas for their patient explanations and review of this tutorial. In addition, J. B. Thomas graciously allowed the use of Fig. 5 and the alternate way of looking at bandwidth synthesis that he drew up for an article to be published in the future.

## References

1. Thomas, J. B., "An Analysis of Long Baseline Radio Interferometry," *The Deep Space Network Progress Report*, Technical Report 32-1526, Volume VIII, Jet Propulsion Laboratory, Pasadena, California, February 1972.
2. Williams, J. G., "Very Long Baseline Interferometry and Its Sensitivity to Geophysical and Astronomical Effects," *Jet Propulsion Laboratory Space Programs Summary 37-62*, Volume II, February 1970.
3. Fanselow, J. L., "Superiority of Bandwidth Synthesis Over the Burst Mode Technique for Determining Time Delay in VLBI," IOM 391.5-517, December 1, 1975 (JPL internal document).
4. Thomas, J. B., "An Analysis of Long Baseline Radio Interferometry, Part III," *The Deep Space Network Progress Report*, Technical Report 32-1526, Volume XVI, Jet Propulsion Laboratory, Pasadena, California, August 1973.
5. Thomas, J. B., "System Noise Effects in VLBI Measurements," Engineering Memorandum 315.6, October 25, 1976 (JPL internal document).
6. Molinder, J. I., and Mulhall, B. D. L., "Minutes of the DSN VLBI Implementation Team Meeting of 16 December 1976," IOM AE-76-197, 17 December 1976 (JPL internal document).
7. Brown, D. S., "VLBI Fringe Phase SNR and Bit Calculations," IOM 315.1-222, 14 December 1977 (JPL internal document).
8. VLBI Validation Report, Pre-Session No. 1, April 1, 1977, Document 890-60 (JPL internal document).
9. Molinder, J. I., and Mulhall, B. D. L., "Minutes of the DSN VLBI Implementation Team Meeting of 20 January 1977," IOM AE-77-11, 24 January 1977 (JPL internal document).
10. Rogers, Alan E. E., "Very Long Baseline Interferometry with Large Effective Bandwidth for Phase-Delay Measurements," *Radio Science*, Volume 5, Number 10, October 1970.
11. Thomas, J. B., "An Analysis of Long Baseline Radio Interferometry, Part II," *The Deep Space Network Progress Report*, Technical Report 35-1526, Volume VIII, Jet Propulsion Laboratory, Pasadena, California, May 1972.

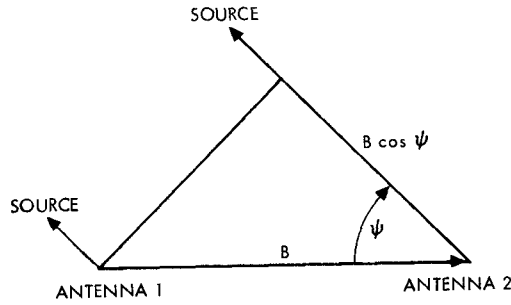
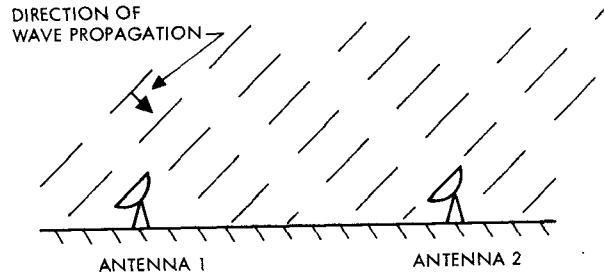
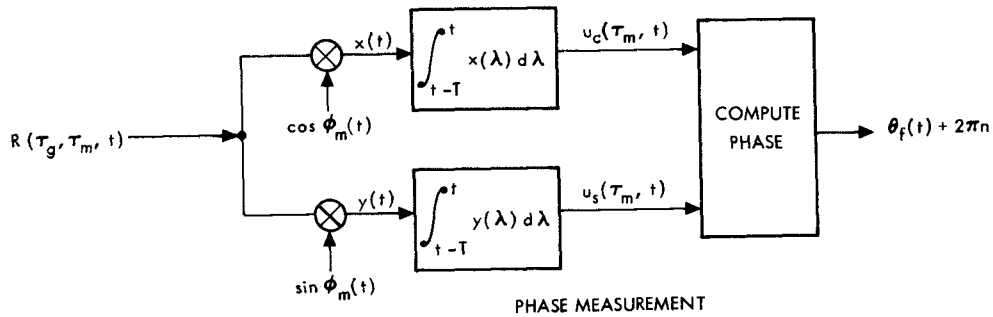
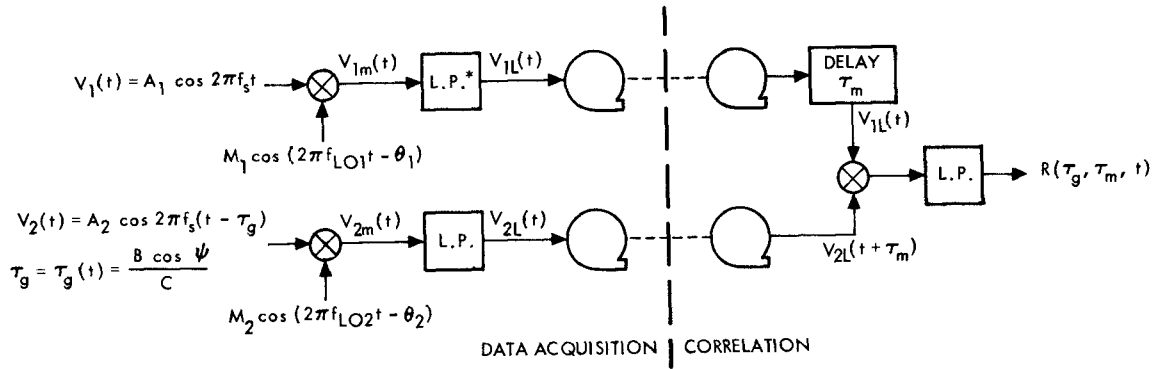


Fig. 1. VLBI Geometry



\*LOW-PASS FILTER

Fig. 2. VLBI signal processing

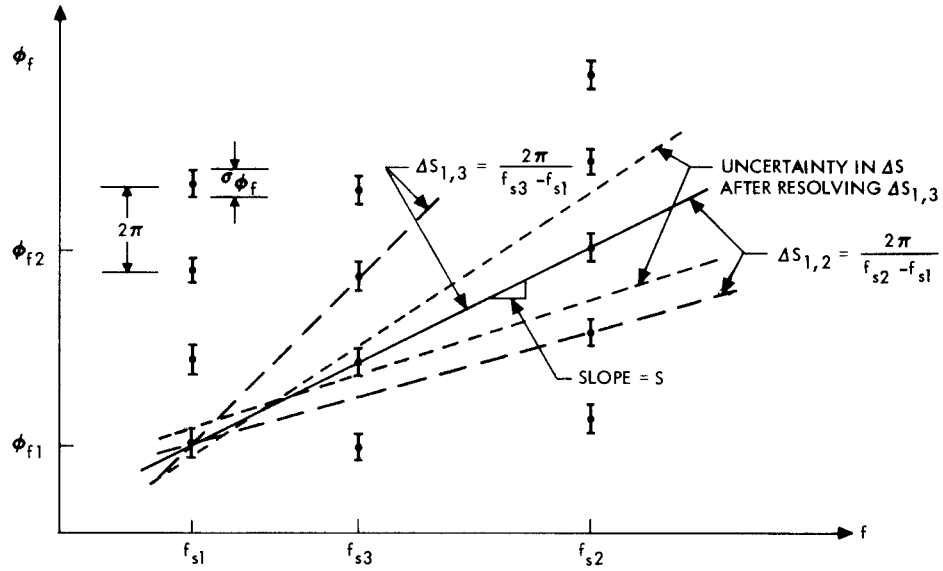


Fig. 3. VLBI relative phase ambiguity resolution and bandwidth synthesis

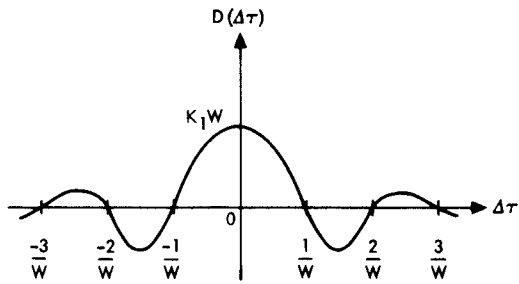


Fig. 4. Amplitude of cross-correlation function  $D(\Delta\tau)$  vs bit stream misalignment ( $\Delta\tau$ )

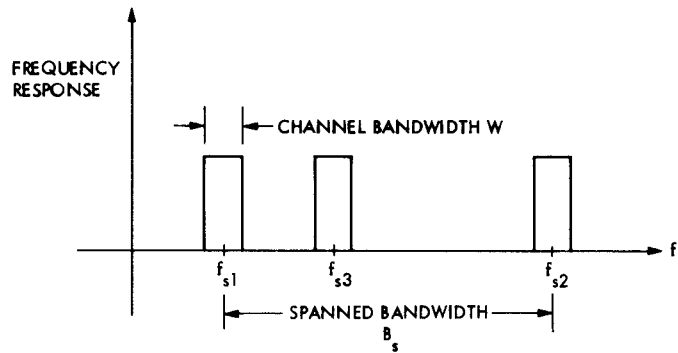


Fig. 5. Frequency response of bandwidth synthesis VLBI system

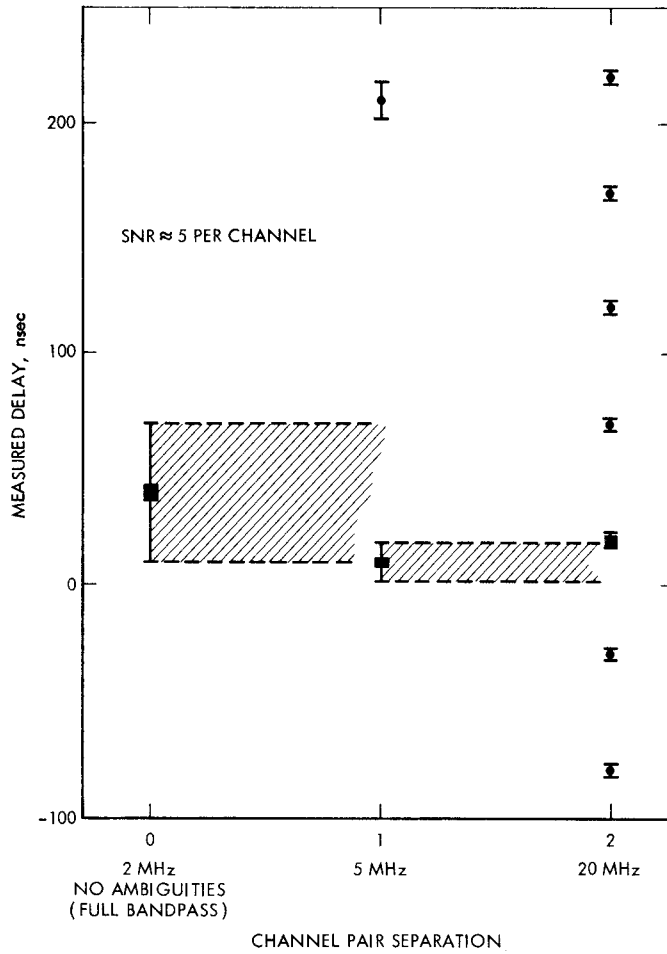


Fig. 6. Schematic example of ambiguity resolution in bandwidth synthesis

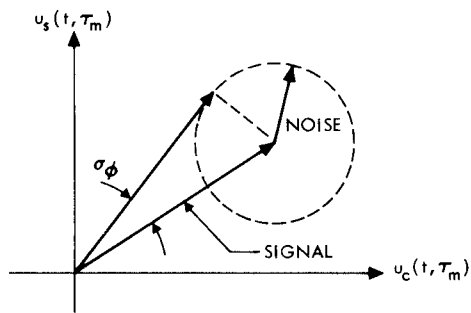


Fig. 7. Effect of noise on accuracy of phase measurement

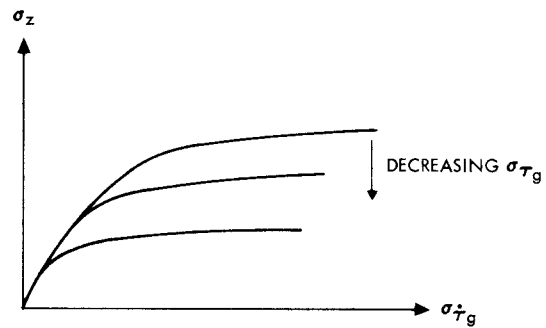


Fig. 8. Standard deviation in Z-component of baseline as a function of  $\sigma_{\tau_g}$  and  $\sigma_{\dot{\tau}_g}$